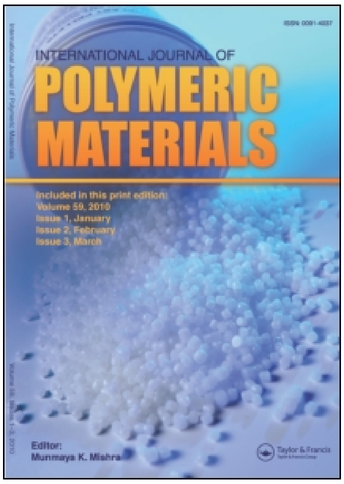

International Journal of Polymeric Materials
Publication details, including instructions for authors and subscription information:
http://www.informaworld.com/smpp/title~content=t713647664

Computer Simulation of Creep and Fracture of Highly Drawn Polymers

M. G. Zaitsev[a]; S. A. Stremyakov[a]; S. A. Gordeev[b]
[a] Moscow Pedagogical State University, Moscow, Russia [b] Research Institute of Synthetic Fibers, Russia

To cite this Article Zaitsev, M. G. , Stremyakov, S. A. and Gordeev, S. A.(1993) 'Computer Simulation of Creep and Fracture of Highly Drawn Polymers', International Journal of Polymeric Materials, 22: 1, 25 — 31

To link to this Article: DOI: 10.1080/00914039308012054

URL: http://dx.doi.org/10.1080/00914039308012054

Intern. J. Polymeric Mater., 1993, Vol. 22, pp. 25–31
Reprints available directly from the publisher
Photocopying permitted by license only

Printed in Malaysia

Computer Simulation of Creep and Fracture of Highly Drawn Polymers

M. G. ZAITSEV and S. A. STREMYAKOV
Moscow Pedagogical State University, 1 M. Pirogovskaya, Moscow 119882, Russia

and

S. A. GORDEEV
Research Institute of Synthetic Fibers, Tver' 170032, Russia

A computer kinetic model was proposed describing creep and fracture of the microfibrilla in the drawn semicrystalline polymer and allowing for the concurrent and interrelated processes of slippage of polymer chains, redistribution of the polymer units between the amorphous regions and chains scissions. A self-consistent system of non-linear kinetic equations for tie chains length distribution function was written and its numerical analysis was made with a computer. As a result, a stress-strain curve for a single microfibrilla and an averaged curve for a high drawn polymer fiber were obtained. Also a portion of tie chains scissions and the concentration of defects in crystallites as a function of fiber deformation were obtained.

KEY WORDS Creep, fracture, high drawn semicrystalline polymers, computer simulation.

INTRODUCTION

Experimental investigation into the structure of drawn polymers under load[1,2] shows that the mechanical properties as well as the kinetics of failure and deformation are largely determined by the structure of the intrafibrillar amorphous regions. For the mechanical processes the most important characteristics of the amorphous region are a portion of tie chains and their length distribution. The length distribution density $\rho(l)$ and the strength of drawn polymers were experimentally found to concur.[3–6] Two models were considered in interpreting the published experimental data. In one model the tie chains were taken as rigidly fixed at the boundary of crystallites.[1,3–7] In the other, slippage of the chains through the crystallite was assumed to take place.[1,2,7] The model of rigidly fixed chains of different length was carefully analyzed in the theoretical studies.[8–10] Pulling out of a part of a single chain from the crystallite was theoretically analyzed in the studies.[11–13] The slippage of the chains through a crystallite, when high stresses are applied to the sample, was experimentally confirmed.[14,15]

The studies presented here describe fiber creep and fracture in drawn polymers based on computer simulation of the evolution of tie chains length density distribution $\rho(l)$ in

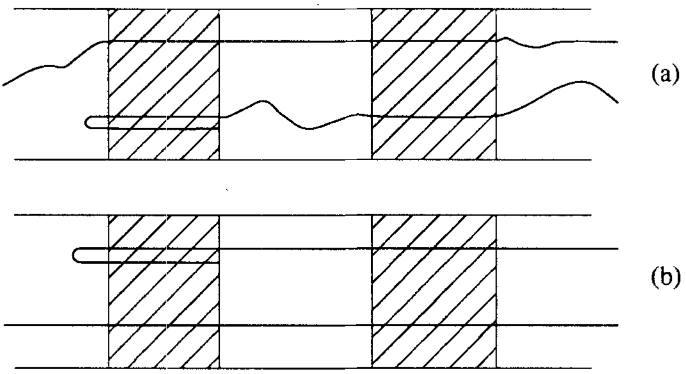

FIGURE 1 Polymer chain in a microfibrilla model for (a) unstressed and (b) stressed chain segments in the adjacent amorphous regions.

microfibrilla amorphous regions with allowance made for interrelated slippage and scission of tie chains occurring concurrently.

MODEL

The kinetic model and the results from the computer simulation of the stretching of a single microfibrilla in drawn polymer were previously described in detail.[16,17]

Let us assume that recrystallization and additional growth of the crystallites do not take place in the course of deformation of the microfibrilla. Thus the evolution of the tie chains length density distribution is governed only by the redistribution of the polymer units between the amorphous regions and by pulling the units out of the crystallites. We also assume that the pulling of one chain unit out of the crystallite and the rupture of the stressed chain are caused by thermal fluctuations. The mean expectation time of these acts is:

$$\tau \sim \exp\left(\frac{u(x)}{kT}\right), \tag{1}$$

where T is the temperature, $u(x)$ is the activation barrier for slippage or scission of the chain which depends on the deformation of the stressed chain segment in the amorphous region (Figure 1). In the present study it is assumed that

$$u(x) = u_0^j\left(1 - \frac{x}{x_{\max}^j}\right), \tag{2}$$

where u_0^j is the activation barrier of slippage or scission for the unstressed chain, $x_{\max}^j$ is the deformation of the chain at which the activation barrier $u(x)$ tends to zero (index j is explained below). The data[11–13] evidence that the pulling of the chain unit out of the crystallite results in the formation therein of the one-dimensional dislocation. There are two possibilities here.

(i) If the chain passes through the crystallite and enters the adjacent amorphous region with the unstressed chain segment (Figure 1a), the dislocation moves through the crystallite and emerging on its opposite surface. This pulls the chain unit of the unstressed chain in the

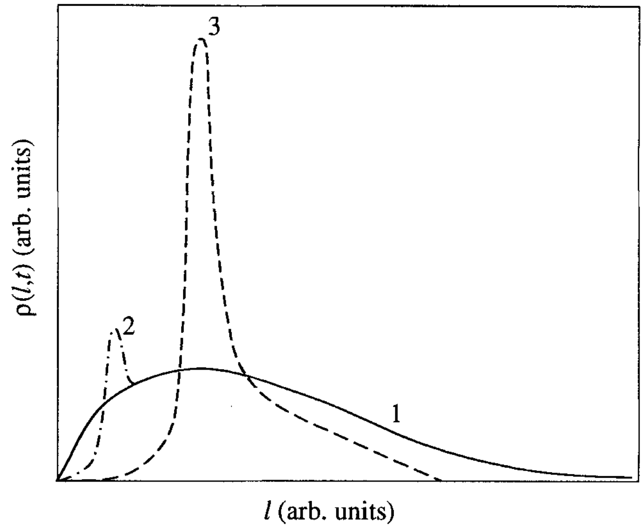

FIGURE 2 Evolution of the tie chains length distribution at $t = 0$ (curve 1), $t = t_1$ (curve 2), $t = t_2$ (curve 3). $t_2 > t_1 > 0$.

adjacent region into the crystallite, i.e. it will result in the redistribution of the polymer units between the regions. As the microfibrilla is stretched further, the process may recur. In such a case, for as long as the chain segment in the adjacent region remains unstressed, the parameters u_0^j and $x_{\max}^j$ of the potential barrier for slippage of the chain remain unchanged. (ii) If the chain segment in the adjacent region is stressed or the chain in the crystallite forms a fold (Figure 1b) the dislocation inside the crystallite ceases. This impedes the pulling of the stressed chain segment in the amorphous region on further stretching of the microfibrilla. The activation barrier and the maximum deformation for each subsequent chain unit pulled out of the crystallite is higher than for the preceding one,[13] i.e. $u_0^j > u_0^{j-1}$, $x_{\max}^j > x_{\max}^{j-1}$ (j is the number of the chain units pull by the stressed chain segment out of the crystallite into the amorphous region).

It is assumed in the model that after k chain units have been pulled out of the crystallite, the barrier for the subsequent extension becomes higher than that of the chain scission. This results in the chain scission. The input parameters of the model are as follows: (i) the activation barriers of slippage and scission in the chain (and their force relationships); (ii) the initial tie chains length density distribution $\rho(l, 0)$. The kinetic equations for $\rho(l, t)$, were given earlier[16] for root-mean square deviations δ of $\rho(l, 0)$, here t is time. It is these equations that form the basis for the computer simulation.

COMPUTER SIMULATION RESULTS

Figure 2 presents the curves of the tie chains length density distribution at various values of microfibrilla deformations (various deformation times in the mode $\dot{\varepsilon} = \text{const}$). It is seen that the slippage of the chains through the crystallite results in a sharp peak on the function $\rho(l, t)$ in the region of the short chains which shifts towards the greater values of length as microfibrilla deformation grows. It is of interest that at medium deformations

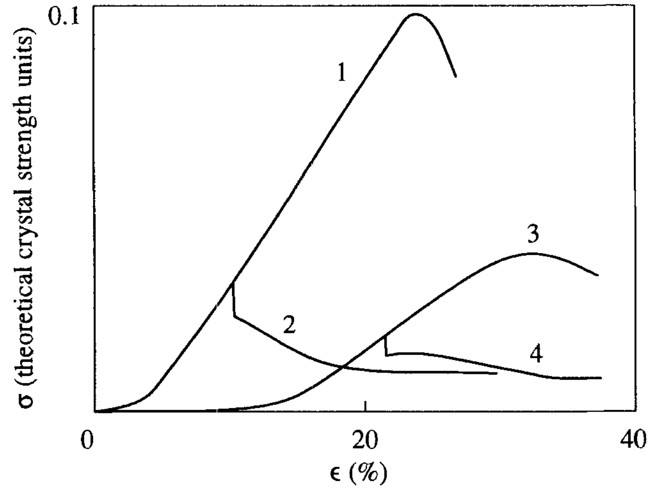

FIGURE 3 Theoretical stress-strain curves: absolutely stable crystallites (curves 1, 3), possible crystallite amorphization (curves 2, 4). Root-mean-square deviations of the $\rho(l,0)$: $\delta = 2.3$ (curves 1, 2), $\delta = 3.6$ (curves 3, 4).

the tie chains length distribution turns out to be bimodal, which agrees with the results of the NMR-experiments.[4] As $\rho(l,t)$ gets narrower, the microfibrilla becomes stronger. However, after the chain pulling out of the crystallite is exhausted, a portion of the chain scissions tends to grow in magnitude. This results in the maximum (or a long plateau) on the relationship $\sigma(\epsilon)$ of the microfibrilla (in the mode $\dot{\epsilon} = \text{const}$, Figure 3). The value of this maximum corresponds to the strength of the microfibrilla at the preset ϵ and initial length distribution $\rho(l,0)$, since at $\epsilon > \epsilon_{\max}$ the fibrilla with equal amorphous regions is unstable and its further stretching results in a rapid localization of fracture in one of the amorphous regions.

The latter result is indisputably true, assuming that the crystallites are quite stable and at any stage of the microfibrilla stretching they ensure the preset potential barriers for pulling the chain units. However, the analysis[17] has revealed another possibility for microfibrilla to lose stability. Accumulation within the crystallites of the one-dimensional dislocations that cannot move onto the crystallite surface may cause amorphization of the crystallites. As a result they will cease acting as "clamps" for chain segments in the amorphous regions. As is seen from Figure 3, the stress-strain curves look different, provided this process is taken into account. The analysis of the data in Reference 17 shows that the fracture of the amorphous regions is realized only in case of wide initial length distributions and high barriers of slippage. In the case of the narrow initial distributions and the barriers characteristic of non-polar intermolecular interactions (specific for highly drawn polyethylene) the fibrilla loses stability due to amorphization of crystallites.

COMPARISON WITH EXPERIMENT

When comparing the results of the computer simulation with the experimental data, account should be taken of the nonuniformity of loading of microfibrillae in the real fiber. Let us assume that the nonuniformity of loading is mainly caused by the scatter of the longitudinal

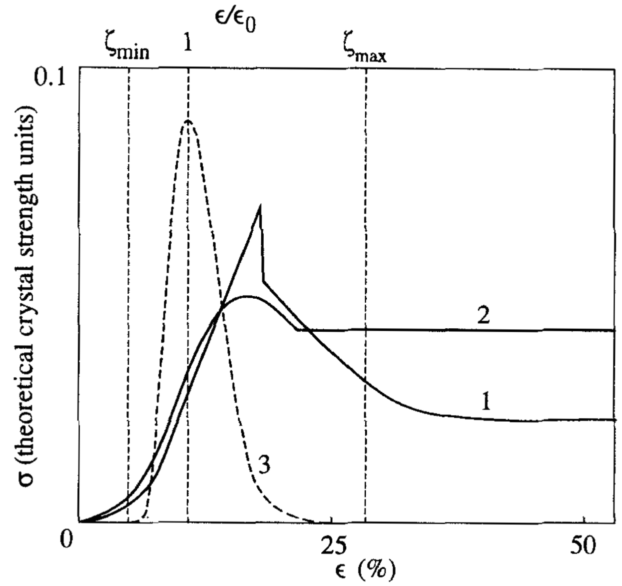

FIGURE 4 Stress-strain curve of an individual microfibrilla at $\delta = 2.3$ (curve 1), average stress-strain curve of a fiber (curve 2), and the example of microfibril strain distribution $f(\epsilon)$ (curve 3).

dimensions of crystallites. Experimental data[18] show that in the drawn polyethylene the dimensions of crystallites are well approximated by Γ-distribution. This allows the assumption that the strain distribution of microfibrillae is Γ-distribution too:

$$f(\epsilon) = \frac{\alpha^{\beta}}{\Gamma(\beta)} \epsilon^{\beta-1} \exp(-\alpha\epsilon), \tag{3}$$

where $\Gamma(\beta)$ is gamma function, α and β are parameters of the distribution ($\alpha > 0$, $\beta > 1$).

The transfer to the description of the process of the fiber stretching is performed by averaging the curve of a single microfibrilla stretching with due regard to the density distribution $f(\epsilon)$.

$$\bar{\sigma}(\epsilon) = \int_{\epsilon_0(1-\xi_{\min})}^{\epsilon_0(1+\xi_{\max})} \sigma(\epsilon) f(\epsilon) \mathrm{d}\epsilon \tag{4}$$

provided that

$$\int_{\epsilon_0(1-\xi_{\min})}^{\epsilon_0(1+\xi_{\max})} f(\epsilon) \mathrm{d}\epsilon = 1,$$

where ϵ_0 corresponds to the value of ϵ in maximum $f(\epsilon)$. Outside the interval ($\xi_{\min}$, $\xi_{\max}$) $f(\epsilon)$ is negligibly small ($|f(\epsilon)| < 10^{-4}$).

Figure 4 shows the stress-strain curve obtained as a result of such averaging. It is obvious that the $\sigma(\epsilon)$ curve flattens revealing the plateau corresponding to the viscous flow of the fiber.

It is natural that the shape of the stress-strain curve is strongly affected by the parameters of the distribution $f(\epsilon)$, which reflects the difference in supermolecular structure

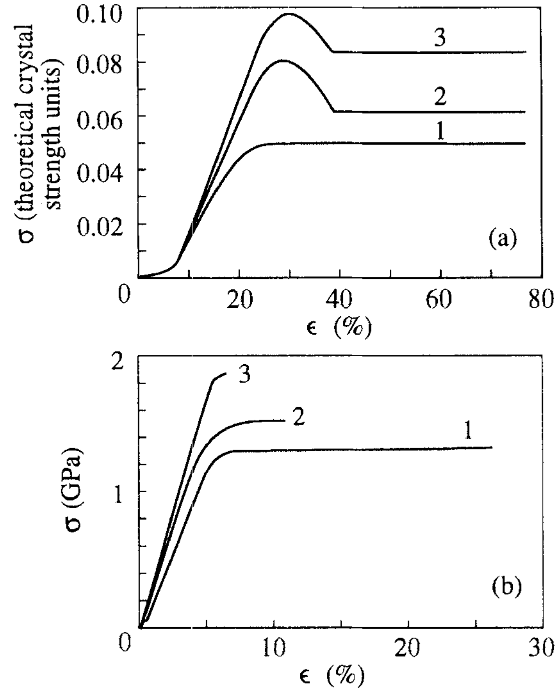

FIGURE 5 (a) Theoretical and (b) experimental stress-strain curves at various deformation rates. $\dot{\epsilon} = 5 \times 10^{-5}\ \mathrm{s}^{-1}$ (curve 1), $\dot{\epsilon} = 5 \times 10^{-4}\ \mathrm{s}^{-1}$ (curve 2), $\dot{\epsilon} = 5 \times 10^{-3}\ \mathrm{s}^{-1}$ (curve 3). Draw ratio $\lambda = 36$.

parameters of the fibers obtained in a different way. Figure 5a shows the calculated stress-strain fiber curves at various rates of deformation. These theoretical results are in good qualitative agreement with the experimental data for polyethylene samples obtained by the gel-technology method (Figure 5b).

Both the experimental and analytical relationships between the strength and the rate of deformation within a wide range of extensions (Figure 6a, b) are represented by parallel straight lines. It is noteworthy that from the viewpoint of the elementary kinetic strength theory the strength-rate of deformation function is described by equation

$$\sigma = \frac{U_0}{\gamma} + \frac{RT}{\gamma}\ln\left(\frac{\dot{\epsilon}}{\dot{\epsilon}_0}\right), \tag{5}$$

where U_0, γ are the parameters of Zhurkov's equation.[1] It is generally assumed that the greater the draw ratio and the narrower the tie chains length distribution, the smaller the value of γ. Thus from the viewpoint of the elementary kinetic strength theory the relationships between σ and $\ln(\dot{\epsilon}/\dot{\epsilon}_0)$ should not be parallel at various draw ratios.

The present study suggests, however, that the failures of the elementary theory should not question the effectiveness of the kinetic approach as such to the description of creep and fracture of highly drawn polymers.

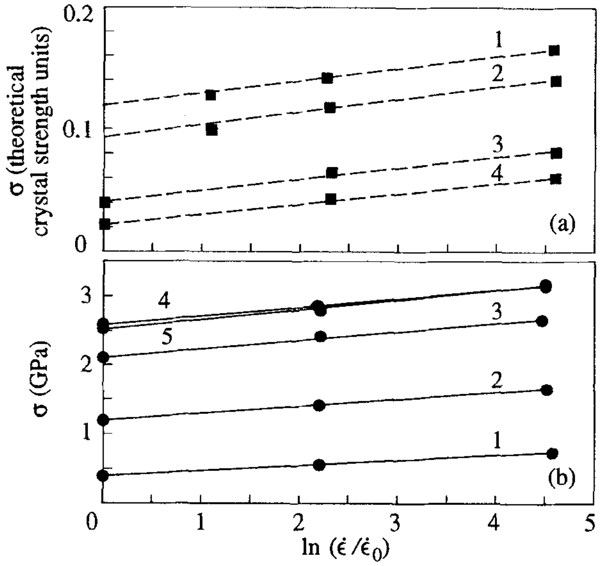

FIGURE 6 Fiber strength-deformation rates curves at $\dot\epsilon_0 = 5.0 \times 10^{-5} s^{-1}$. (a) Theory $\delta = 0.2$ (curve 1), $\delta = 0.7$ (curve 2), $\delta = 2.3$ (curve 3), $\delta = 3.6$ (curve 4); (b) Experiment, $\lambda = 12$ (curve 1), $\lambda = 24$ (curve 2), $\lambda = 36$ (curve 3), $\lambda = 48$ (curve 4), $\lambda = 60$ (curve 5).

References

1. V. R. Regel, A. I. Slutsker, and E. E. Tomashevskii, *Kinetic Nature of Strength of Solids*, (Nauka, Moscow, 1974), (in Russian).
2. H. H. Kausch, *Polymer Fracture*, (Springer-Verlag Berlin; Heidelberg, New-York, 1978).
3. V. V. Zhizhenkov, E. A. Egorov, V. A. Marikhin, and L. P. Myasnikova, *Mechanics of Composits*, **2** 354, (1985), (in Russian).
4. E. A. Egorov, V. V. Zhizhenkov, V. A. Marikhin, L. P. Myasnikova, L. A. Gann, and V. P. Budtov, *Polym. Sci. USSR*, **27**, 1834 (1985).
5. P. M. Pakhomov, M. V. Shablygin, Ye. S. Tsobkallo, and A. S. Cheglova, *Polym. Sci. USSR*, **28**, 621 (1986).
6. K. L. De Vries, B. A. Lloyd, and M. L. Williams, *J. Appl. Phys.*, **42**, 4644 (1971).
7. M. G. Zaitsev, E. A. Egorov, V. V. Zhizhenkov, S. A. Stremyakov, and I. V. Razumovskaya, *Polym. Sci. USSR*, **28**, 226 (1986).
8. A. D. Chevychelov, *Mechanics of Polymers*, **1**, 8 (1967), (in Russian).
9. G. B. Manelis, Ye. V. Polianchik, and L. P. Smirnov, *Polym. Sci. USSR*, **20**, 146 (1978).
10. M. G. Zaitsev, *Polym. Sci. USSR*, **27**, 2802 (1985).
11. A. D. Chevychelov, *Polym. Sci. USSR*, **8**, 49 (1966).
12. H. H. Kausch and D. Langbein, *J. Polym. Sci.*, **11**, 1201 (1973).
13. V. A. Kosobukin and A. D. Chevychelov, *Mechanics of Polymers* **5**, 771 (1973) (in Russian).
14. A. I. Slutsker, A. I. Savitskii, K. Ismonkulov, and A. A. Sidorovitch, *Polym. Sci. USSR*, **28**, 156 (1986).
15. A. I. Slutsker, A. I. Savitskii, K. Ismonkulov, and A. A. Sidorovitch, *Polym. Sci. USSR*, **28**, 1091 (1986).
16. M. G. Zaitsev, S. A. Stremyakov, and I. V. Razzumovskaya, *Polym. Sci. USSR*, **30**, 1457 (1988).
17. M. G. Zaitsev and S. A. Stremyakov, *Polym. Sci. USSR*, **31**, 2017 (1989).
18. G. J. Frye, I. M. Ward, M. G. Dobb, and D. J. Johnson, *J. Polym. Sci., Polym. Phys. Ed.*, **20**, 1677 (1982).